

ON ℓ_1 DATA FITTING AND NONCONVEX NONSMOOTH REGULARIZATION FOR IMAGE RECOVERY

MILA NIKOLOVA*, MICHAEL K. NG[†], AND CHI-PAN TAM[‡]

Abstract. In this paper, we propose cost functions for signal and image recovery composed of ℓ_1 data fitting and nonconvex nonsmooth regularization. The contribution of this paper is to exhibit when and how to employ such cost functions. Our theoretical results show that the solution of the ℓ_1 data fitting and nonconvex nonsmooth minimization problem is such that *all the given data samples* are involved in an exact data fitting component of the data term or in a null component of the regularization part. This is a strong and particular property that can be useful for various image recovery problems. However, the practical interest of the ℓ_1 data fitting and nonconvex nonsmooth minimization is limited by the difficulty of its computational task. Hence the next goal of this paper is to develop a fast minimization algorithm to solve this difficult minimization problem. Our experimental results show that the effectiveness of the proposed algorithm. Illustrations and numerical experiments give a flavor of the possibilities offered by the solutions of cost functions composed of ℓ_1 data fitting and nonconvex nonsmooth regularization.

Key words. Image recovery, Inverse problems, Non-smooth and non-convex analysis, Non-smooth and non-convex optimization, Regularization, ℓ_1 data fitting

1. Introduction. Digital image restoration and reconstruction plays an important part in various applied areas such as medical and astronomical imaging, film restoration, image and video coding and many others [16, 13]. We focus on the common data production model where the observed data $v \in \mathbb{R}^q$ are related to the underlying $n \times m$ image, rearranged into a vector $u \in \mathbb{R}^p$ ($p = mn$), according to a linear model under perturbations

$$v = Au \odot n, \tag{1.1}$$

where $n \in \mathbb{R}^q$ are the perturbations and “ \odot ” represents the way in which n corrupts the data, and A is a $q \times p$ matrix which can for instance be the identity Id or representing optical blurring, distortion wavelets in seismic imaging and nondestructive evaluation, a Radon transform in X-ray tomography, a Fourier transform in diffraction tomography. In noise models, a Gaussian noise can be considered to added to corrupt the data, or an impulsive noise can be considered to be multiplied to corrupt the data, see [16].

In most of the applications, the information provided by the forward model (1.1) alone is not sufficient to find an acceptable solution u . Prior information on the underlying image is needed to restore a convenient u – which is close to data production model (1.1) and satisfies some prior requirements. A flexible means to define such a solution is regularization, see e.g. [4, 7, 12, 1], where u is a minimizer of a cost function of the form

$$\Theta(Au - v) + \beta\Phi(u). \tag{1.2}$$

*Mila Nikolova is with Centre de Mathématiques et de Leurs Applications, (CMLA), ENS Cachan, CNRS, UniverSud, 61 Avenue du Président Wilson, F-94230 Cachan Cedex, France. (nikolova@cmla.ens-cachan.fr)

[†]The Corresponding Author. Michael K. Ng is with the Centre for Mathematical Imaging and Vision and Department of Mathematics, Hong Kong Baptist University, Kowloon Tong, Hong Kong (mng@math.hkbu.edu.hk). The research of this author is supported in part by Hong Kong Research Grants Council Grant and and HKBU FRGs.

[‡]Chi-Pan Tam is with the Centre for Mathematical Imaging and Vision and Department of Mathematics, Hong Kong Baptist University, Kowloon Tong, Hong Kong. (cptam@math.hkbu.edu.hk)

In this expression, Θ forces closeness to data according to (1.1), Φ embodies the priors and $\beta > 0$ is a parameter that controls the trade-off between these two terms. The most usual choice for Θ is $\Theta(v) = \|v\|_2^2$. Since [22, 9, 15], data terms $\Theta(v) = \|v\|_1$ were shown to be useful if some data entries have to be satisfied exactly. Such a property is precious, for instance if n is impulse noise [23, 3] or in image decomposition [2], or in hybrid restoration methods [8]. In this paper, we focus on ℓ_1 data fitting:

$$\sum_{i \in I} |\langle a_i, u \rangle - v[i]| \quad (1.3)$$

$$I = \{1, \dots, q\}$$

where the i th row of A is the transpose of a_i , namely $a_i^T \in \mathbb{R}^{1 \times p}$, $\langle a_i, u \rangle$ refers to the inner product between a_i and u .

In many image processing applications, the regularization Φ reads

$$\Phi(u) = \sum_{j \in J} \varphi(\|G_j u\|_2), \quad (1.4)$$

$$J = \{1, \dots, r\}$$

where for any $j \in J$, $G_j : \mathbb{R}^p \rightarrow \mathbb{R}^s$ for s an integer $s \geq 1$, are linear operators. For instance, the family $\{G_j\} \equiv \{G_j : j \in J\}$ can represent the discrete approximation of the gradient or the Laplacian operator on u , or finite differences of various orders, or the combination of any of these with the synthesis operator of a frame transform. Let us denote by G the matrix where all G_j are vertically concatenated, i.e.,

$$G = [G_1^T, \dots, G_r^T]^T,$$

where the superscript stands for transpose.

The function $\varphi : \mathbb{R} \mapsto \mathbb{R}_+$ is called a potential function (PF). Various potential functions (PFs) φ have been used in the literature, a review can be found for instance in [5]. An important requirement is that φ allows the recovery of large differences $|d_j f|_2$ at the locations of edges and smooth the other differences. It is well known that this requirement cannot be met by $\varphi(t) = t^2$ which was originally used in [29]. Since the pioneering work of Geman & Geman [12], different non-convex functions φ have been considered either in a statistical or in a variational framework, see e.g. [4, 10, 11, 18, 19]. In order to avoid the numerical intricacies arising with nonconvex regularization, since [14, 17, 28] in 1990, an important effort was done to derive convex edge-preserving PFs, see [1] for an excellent account. Nevertheless, nonconvex nonsmooth regularization offers much richer possibilities to restore high quality images with neat edges: for regularizer functions of the form (1.4) a theoretical explanation was provided in [24] while numerical examples can be found in numerous articles, see e.g. [10, 11, 21, 27, 25]. However, to the best of our knowledge, there is no results explaining cases when *nonconvex nonsmooth regularization* is combined with ℓ_1 (*nonsmooth, convex*) data fitting.

This paper provides two main contributions. The theoretical one is to prove that the minimizers \hat{u} of energies of the form (1.2), (1.3) and (1.4), where $\varphi(\|\cdot\|_2)$ is nonconvex and nonsmooth at zero, are such that each one of its entries $\hat{u}[k]$ is involved at least in one $i \in I$ such that $a_i[k] \neq 0$ and $\langle a_i, \hat{u} \rangle = 0$ or one $j \in J$ such that for some $\ell \in \{1, \dots, s\}$ one has $G_j^\ell[k] \neq 0$ and $\|G_j \hat{u}\|_2 = 0$. In the simple case when $A = \text{Id}$ and $\{G_j\}$ are discrete gradients or first-order differences, minimizers are composed of (i) constant regions surrounded by closed contours and (ii) restored

samples fitting observed samples exactly (i.e. equal to them). Theoretical results are outlined in Section 2. We also derive fast algorithms to approximate faithfully the global minimizer of these nonconvex and nonsmooth energies (Section 3). Our experimental results (Section 4) show clearly the effectiveness and efficiency of the proposed numerical schemes, as well as the interest for image recovery of the proposed energies. Concluding remarks are given in Section 5.

2. Properties of Minimizers. In this section, we study the property of minimizers of

$$\mathcal{F}(u) = \|Au - v\|_1 + \beta\Phi(u) \tag{2.1}$$

where Φ is of the form (1.4). We adopt the usual assumption that

H1. $\ker A \cap \ker G = \{0\}$.

We will also suppose that

H2. For any subset $\tilde{I} \subset I$ with $\tilde{I} \neq \emptyset$, we have

$$w \in \ker(G) \Rightarrow \exists i \in \tilde{I} \text{ such that } \langle a_i, w \rangle \neq 0.$$

This assumption might seem tricky. Nevertheless it holds true in the majority of cases encountered in practice. E.g., it is true for all A mentioned in the introduction when $\{G_i\}$ involves some kind of difference or discrete differential operators.

H3. For any $j \in J$, we have $G_j \neq 0$.

The last H3 and is just a common sense trivial requirement.

The function $t \rightarrow \varphi(|t|)$ is *nonconvex and nondifferentiable at zero*. It is often called a potential function (PF). The precise assumptions on φ are listed below.

H4. $\varphi : \mathbb{R}_+ \rightarrow \mathbb{R}_+$ is \mathcal{C}^2 on \mathbb{R}_+^* and $\varphi(t) > \varphi(0) = 0, \forall t > 0$;

H5. $\varphi'(0^+) > 0$ and $\varphi'(t) > 0$ on \mathbb{R}_+^* .

H6. φ'' is increasing on \mathbb{R}_+^* , $\varphi''(t) < 0, \forall t > 0$ and $\lim_{t \searrow 0} \varphi''(t) < 0$ is well defined and finite.

Note that the condition that $\lim_{t \searrow 0} \varphi''(t) < 0$ is well defined in H6 implies that $\varphi'(0^+) > 0$ in H5 is finite. Several examples of functions φ satisfying all assumptions H4, H5 and H6 are shown in Table 2.1 and plotted in Fig. 2.1.

	(f1)	(f2)	(f3)	(f4)
$\varphi(t)$	$\frac{\alpha t}{\alpha t + 1}$ $\alpha > 0$	$1 - \alpha^t$ $0 < \alpha < 1$	$\ln(\alpha t + 1)$ $\alpha > 0$	$(t + \varepsilon)^\alpha - \varepsilon^\alpha$ $0 < \alpha < 1, \varepsilon > 0$
$\varphi'(t)$	$\frac{\alpha}{(\alpha t + 1)^2}$	$-\alpha^t \ln \alpha > 0$	$\frac{\alpha}{\alpha t + 1}$	$\alpha(t + \varepsilon)^{\alpha-1}$
$\varphi'(0^+)$	α	$-\ln \alpha > 0$	α	$\alpha \varepsilon^{\alpha-1}$
$\varphi''(t)$	$\frac{-2\alpha^2}{(\alpha t + 1)^3}$	$-\alpha^t (\ln \alpha)^2$	$\frac{-\alpha^2}{(\alpha t + 1)^2}$	$\alpha(\alpha - 1)(t + \varepsilon)^{\alpha-2} < 0$
$\lim_{t \searrow 0} \varphi''(t)$	$-2\alpha^2$	$-(\ln \alpha)^2$	$-\alpha^2$	$\alpha(\alpha - 1)\varepsilon^{\alpha-2} < 0$

TABLE 2.1

Functions $\varphi : \mathbb{R}_+ \rightarrow \mathbb{R}_+$ satisfying H4, H5 and H6.

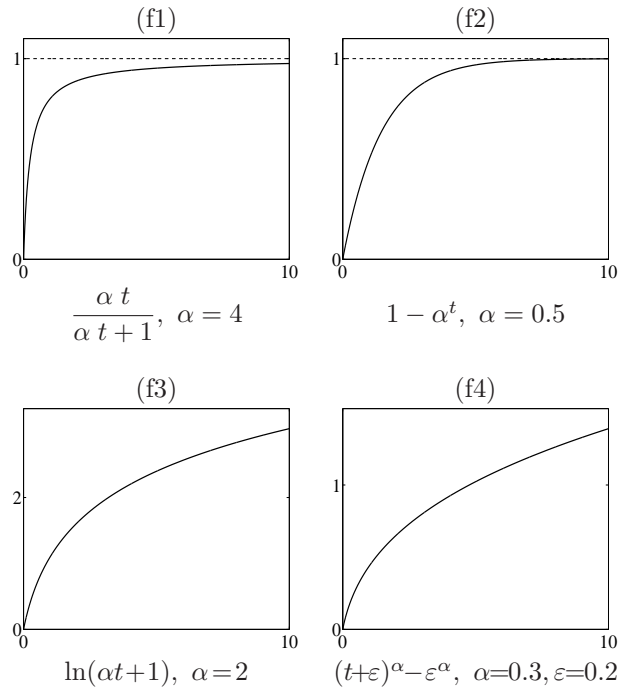


FIG. 2.1. Plots of the PFs φ given in Table 2.1. Note that (f1) and (f2) are bounded above, which is not the case for (f3) and (f4).

2.1. Motivation. Two illustrations of minimizers of \mathcal{F} in (2.1) for $A = \text{Id}$, $\{G_j\}$ first-order differences (hence H1, H2 and H3 hold) and a φ satisfying all assumptions H4, H5 and H6 are given in Fig. 2.2. One observes that restored samples either fit data samples exactly or form constant patches. Moreover, we see that when β decreases the number of data samples that are fitted exactly increases whereas when β increases more piecewise constant structures are recovered.

EXAMPLE 1 (scalar case). This example is quite illuminating. Given $v \neq 0$, consider the pair of functions given below

$$\mathcal{F}(u) = |u - v| + \beta\varphi(|u|) \quad \text{for} \quad \varphi(u) = \frac{\alpha u}{1 + \alpha u}, \forall u \in \mathbb{R}, \quad (2.2)$$

$$F(u) = \mathcal{F}(u), \quad \forall u \in \mathbb{R} \setminus \{0, v\}. \quad (2.3)$$

Note that F is the restriction of \mathcal{F} on $\mathbb{R} \setminus \{0, v\}$, and that φ is the PF (f1) in Table 2.1 meets all H4, H5 and H6.

As usual, we denote by $D_k^j f$ the differential of order j of a function f with respect to its k -th argument.

Let \hat{u} be a minimizer of \mathcal{F} . The necessary conditions for \mathcal{F} to have a (local) minimum at $\hat{u} \neq 0$ and $\hat{u} \neq v$, or equivalently, for F to have a (local) minimum at \hat{u} , namely $D\mathcal{F}(\hat{u}) = 0$ and $D^2\mathcal{F}(\hat{u}) \geq 0$, do not hold:

$$\begin{aligned} D\mathcal{F}(\hat{u}) &= DF(\hat{u}) = \text{sign}(\hat{u} - v) + \beta\varphi'(|\hat{u}|)\text{sign}(\hat{u}) = 0 \\ D^2\mathcal{F}(\hat{u}) &= D^2F(\hat{u}) = \beta\varphi''(|\hat{u}|) < 0, \end{aligned}$$

where the last inequality comes from the concavity of φ on \mathbb{R}_+^* , see H6. Hence there is no minimizer such that $\hat{u} \neq 0$ and $\hat{u} \neq v$. In this way, F in (2.3) does not have

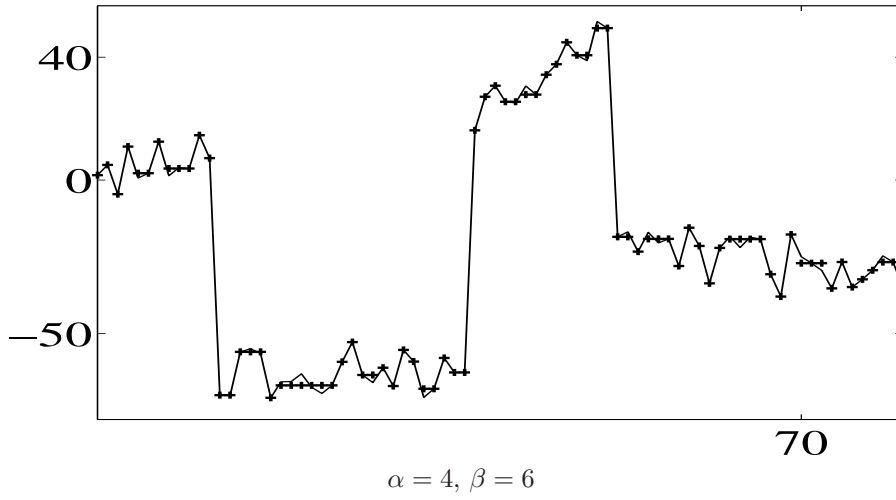
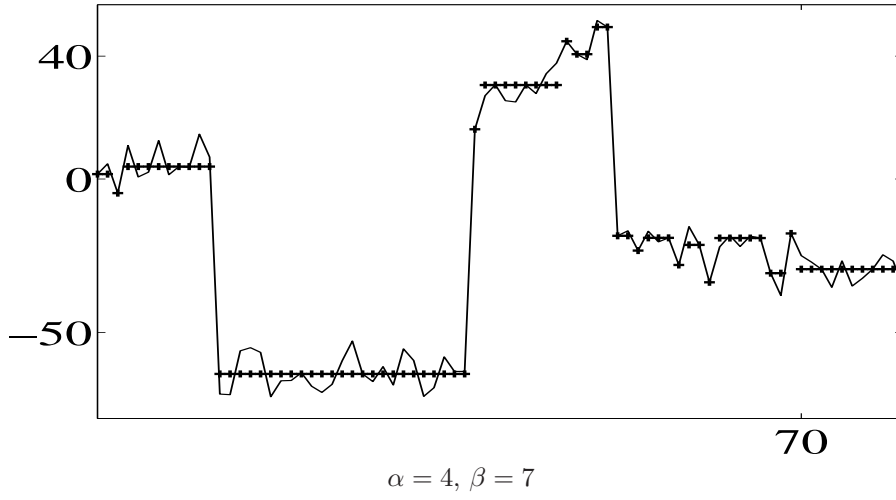


FIG. 2.2. $\mathcal{F}(u) = \|u - v\|_1 + \beta \sum_{i=1}^{p-1} \varphi(|u[i+1] - u[i]|)$ for $\varphi(t) = \frac{\alpha t}{\alpha t + 1}$. Data v (—), each sample of the minimizer \hat{u} is marked with +.

minimizers. Hence any minimizer of \mathcal{F} in (2.2) satisfies

$$\hat{u} \in \{0, v\}.$$

More precisely,

$$\begin{aligned} \hat{u}_1 = 0 &\Rightarrow \mathcal{F}(\hat{u}_1) = |v| \\ \hat{u}_2 = v &\Rightarrow \mathcal{F}(\hat{u}_2) = \beta \varphi(|v|) = \mathcal{F}(\hat{u}_2) = \beta \frac{\alpha |v|}{1 + \alpha |v|}. \end{aligned}$$

Hence the global minimizer \hat{u} is:

$$\begin{aligned} \hat{u} = \hat{u}_1 = 0 & \text{ if } \mathcal{F}(\hat{u}_1) < \mathcal{F}(\hat{u}_2) \Leftrightarrow |v| < \beta \frac{\alpha|v|}{1 + \alpha|v|} \Leftrightarrow |v| < \beta - \frac{1}{\alpha} \\ \hat{u} = \{0, v\} & \Leftrightarrow \mathcal{F}(\hat{u}_1) = \mathcal{F}(\hat{u}_2) \Leftrightarrow |v| = \beta - \frac{1}{\alpha} \\ \hat{u} = \hat{u}_2 = v & \text{ if } \mathcal{F}(\hat{u}_1) > \mathcal{F}(\hat{u}_2) \Leftrightarrow |v| > \beta - \frac{1}{\alpha} \end{aligned}$$

2.2. Preliminary results. When are we sure that our nonconvex nonsmooth energies \mathcal{F} do have minimizers?

REMARK 1. *We consider that φ satisfies H4, H5 and H6. Let one of the following assumptions hold:*

- (a) $\text{rank}(A) = p$;
- (b) *H1 holds and $\lim_{t \rightarrow \infty} \varphi(t) = +\infty$.*

Then for any v , we obviously have

$$\lim_{\|u\| \rightarrow \infty} \mathcal{F}(u) = +\infty, \quad \forall u \in \mathbb{R}^p.$$

This, combined with the fact that \mathcal{F} is a continuous function guarantees that $\forall v \in \mathbb{R}^q$ the function \mathcal{F} in (2.1) does admit a minimum; see e.g. [6].

Note that the PFs (f3) and (f4) given in Table 2.1 satisfy the assumption on φ in condition (b) above. We should emphasize that Remark 1 gives only sufficient conditions for the existence of a minimizer. They are not necessary, as it can be easily checked (e.g. by hand, using simple 3-pixel examples). We will not discuss furthermore the question of existence of minimizers.

Given $v \in \mathbb{R}^q$, let \hat{u} be a (local) minimizer of \mathcal{F} . With each such \hat{u} we systematically associate the following subsets:

$$\widehat{I}_0 = \{i \in I : \langle a_i, \hat{u} \rangle = v[i]\} \quad \text{and} \quad \widehat{I}_0^c = I \setminus \widehat{I}_0 = \{i \in I : \langle a_i, \hat{u} \rangle \neq v[i]\} \quad (2.4)$$

$$\widehat{J}_0 = \{i \in J : \|\mathbf{G}_i \hat{u}\|_2 = 0\} \quad \text{and} \quad \widehat{J}_0^c = J \setminus \widehat{J}_0 = \{i \in J : \|\mathbf{G}_i \hat{u}\|_2 \neq 0\} \quad (2.5)$$

Note that \widehat{J}_0 equivalently reads

$$\widehat{J}_0 = \{i \in J : \mathbf{G}_i \hat{u} = 0 \in \mathbb{R}^s\}. \quad (2.6)$$

For $(u, v) \in \mathbb{R}^p \times \mathbb{R}^q$, denote

$$\psi_i(u) = |\langle a_i, u \rangle - v[i]|, \quad i \in I, \quad (2.7)$$

$$\phi_i(u) = \varphi(\|\mathbf{G}_i u\|_2), \quad i \in J. \quad (2.8)$$

LEMMA 2.1. *Given $v \in \mathbb{R}^q$, let \mathcal{F} reach a (local) minimum at \hat{u} . Let the assumptions H4 and H5 hold. Put*

$$\rho = \min \left\{ \min_{i \in \widehat{I}_0^c} \frac{|\langle a_i, \hat{u} \rangle - v[i]|}{\|a_i\|_2}, \min_{j \in \widehat{J}_0^c} \frac{\|\mathbf{G}_j \hat{u}\|_2}{\|\mathbf{G}_j\|_2} \right\}.$$

Clearly $\rho > 0$. Let $u \in B(\hat{u}, \rho) \stackrel{\text{def}}{=} \{w \in \mathbb{R}^p : \|w - \hat{u}\|_2 < \rho\}$ then

$$i \in \widehat{I}_0^c \Rightarrow \psi_i(u) \in \mathcal{C}^2(B(\hat{u}, \rho)) \quad (2.9)$$

$$j \in \widehat{J}_0^c \Rightarrow \phi_j(u) \in \mathcal{C}^2(B(\hat{u}, \rho)) \quad (2.10)$$

In words, $\psi_i, \forall i \in \widehat{I}_0^c$ and $\phi_j, \forall j \in \widehat{J}_0^c$, as given in (2.7) and (2.8), respectively, are \mathcal{C}^2 smooth on the open ball $B(\hat{u}, \rho)$.

Proof. Notice that $u \in B(\hat{u}, \rho)$ is equivalent to $u = \hat{u} + w$ for $\|w\|_2 < \rho$. Therefore, we consider an arbitrary $w \in B(0, \rho)$.

Since $\rho \leq \min_{i \in \widehat{I}_0^c} \frac{|\langle a_i, \hat{u} \rangle - v[i]|}{\|a_i\|_2}$, we have $\|w\|_2 < \min_{i \in \widehat{I}_0^c} \frac{|\langle a_i, \hat{u} \rangle - v[i]|}{\|a_i\|_2}$. Using this fact, we have the following inequality chain:

$$\begin{aligned} i \in \widehat{I}_0^c &\Rightarrow \psi_i(\hat{u} + w) = |\langle a_i, \hat{u} + w \rangle - v[i]| \geq |\langle a_i, \hat{u} \rangle - v[i]| - |\langle a_i, w \rangle| \\ &\geq |\langle a_i, \hat{u} \rangle - v[i]| - \|a_i\|_2 \|w\|_2 \\ &= \|a_i\|_2 \left(\frac{|\langle a_i, \hat{u} \rangle - v[i]|}{\|a_i\|_2} - \|w\|_2 \right) \\ &\geq \|a_i\|_2 \left(\min_{i \in \widehat{I}_0^c} \frac{|\langle a_i, \hat{u} \rangle - v[i]|}{\|a_i\|_2} - \|w\|_2 \right) > 0. \end{aligned}$$

Hence (2.9).

Using that $\rho \leq \min_{j \in \widehat{J}_0^c} \frac{\|G_j \hat{u}\|_2}{\|G_j\|_2}$, we get $\|w\|_2 < \min_{j \in \widehat{J}_0^c} \frac{\|G_j \hat{u}\|_2}{\|G_j\|_2}$. Furthermore,

$$\begin{aligned} j \in \widehat{J}_0^c &\Rightarrow \|G_j(\hat{u} + w)\|_2 \geq \|G_j \hat{u}\|_2 - \|G_j w\|_2 \geq \|G_j \hat{u}\|_2 - \|G_j\|_2 \|w\|_2 \\ &= \|G_j\|_2 \left(\frac{\|G_j \hat{u}\|_2}{\|G_j\|_2} - \|w\|_2 \right) \\ &\geq \|G_j\|_2 \left(\min_{j \in \widehat{J}_0^c} \frac{\|G_j \hat{u}\|_2}{\|G_j\|_2} - \|w\|_2 \right) > 0. \end{aligned}$$

Combining this result with the fact that φ in (2.8) is \mathcal{C}^2 on \mathbb{R}_+^* by H4 leads to (2.10). \square

2.3. Exact fitting results. We will start by presenting the main result of this subsection.

Given $w \in \mathbb{R}^p$ or $w \in \mathbb{R}^{1 \times p}$, we use the classical notation

$$\text{supp}(w) = \{k \in \{1, \dots, p\} : w[k] \neq 0\}.$$

For any $j \in J$, we denote $G_j^\ell \in \mathbb{R}^{1 \times p}$, $1 \leq \ell \leq s$ whenever $s \geq 2$.

THEOREM 2.2. *Consider \mathcal{F} of the form (2.1). Let all assumptions, H1, H2, H3, H4, H5 and H6, hold. If $s \geq 2$, we add assumptions (a) and (b) of Proposition 2.4 below (see p. 9). For $v \in \mathbb{R}^q \setminus \{0\}$, let \hat{u} be a (local) minimizer of \mathcal{F} . Then*

$$1 \leq k \leq p \Rightarrow \begin{cases} \exists i \in I & \text{such that } k \in \text{supp}(a_i) \text{ and } \langle a_i, \hat{u} \rangle = v[i], \\ & \text{or} \\ \exists j \in J, 1 \leq \ell \leq s & \text{such that } k \in \text{supp}(G_j^\ell) \text{ and } G_j \hat{u} = 0. \end{cases} \quad (2.11)$$

Moreover, the minimum reached by \mathcal{F} at \hat{u} is strict.

Using the definitions of \widehat{I}_0 and \widehat{I}_0 as given in (2.4) and (2.5), respectively, a more compact way to state (2.11) is:

$$\begin{aligned} k \in \{1, \dots, p\} &\Rightarrow \\ \exists i \in \widehat{I}_0 &\text{ with } k \in \text{supp}(a_i) \text{ or } \exists j \in \widehat{J}_0, \exists \ell \in \{1, \dots, s\} \text{ with } k \in \text{supp}(G_j^\ell), \end{aligned}$$

where we use the notations introduced in (2.4)-(2.5). Note that k in (2.11) can belong to both $\text{supp}(a_i)$ and $\text{supp}(G_j^\ell)$. In the simple case when $\{a_i, i = 1, \dots, p\}$ is the canonical basis of \mathbb{R}^p (i.e. $A = \text{Id}$) and G_j yield either discrete gradients or first-order finite differences between adjacent samples, the result stated in (2.11) means that a (local) minimizer is composed partly of constant patches, partly of pixels that fit data samples exactly, as seen e. g. in Fig. 2.2.

The proof of the theorem is outlined later on (see p. 12). It involves a series of intermediate results that are presented next.

Given $v \in \mathbb{R}^q$ and \hat{u} —a (local) minimizer of \mathcal{F} —we adopt the notations in (2.4), (2.5) and define the manifolds below:

$$\mathcal{K}_{\hat{u}} = \{w \in \mathbb{R}^p : \langle a_i, w \rangle = v[i], \forall i \in \hat{I}_0 \text{ and } G_i w = 0, \forall i \in \hat{J}_0\}, \quad (2.12)$$

$$K_{\hat{u}} = \{w \in \mathbb{R}^p : \langle a_i, w \rangle = 0, \forall i \in \hat{I}_0 \text{ and } G_i w = 0, \forall i \in \hat{J}_0\}. \quad (2.13)$$

Since

$$\hat{u} \in \mathcal{K}_{\hat{u}},$$

we are guaranteed that $\mathcal{K}_{\hat{u}}$ is nonempty. Note that $K_{\hat{u}}$ is the vector subspace tangent to $\mathcal{K}_{\hat{u}}$.

Given $v \in \mathbb{R}^q$, we will focus on the following function:

$$F : \mathcal{K}_{\hat{u}} \mapsto \mathbb{R} \\ F(u) = \sum_{i \in \hat{I}_0^c} |\langle a_i, u \rangle - v[i]| + \beta \sum_{j \in \hat{J}_0^c} \varphi(\|G_j u\|_2). \quad (2.14)$$

LEMMA 2.3. *Let H2 and H3 hold. We posit the definitions of \hat{I}_0^c and \hat{J}_0^c , see (2.4)-(2.5), as well as the one of $K_{\hat{u}}$ in (2.13). Assume that the dimension of $K_{\hat{u}}$ satisfies $\dim(K_{\hat{u}}) \geq 1$. Then*

$$w \in K_{\hat{u}} \Rightarrow \hat{J}_0^c(w) \stackrel{\text{def}}{=} \{j \in \hat{J}_0^c : \|G_j w\|_2 \neq 0\} \neq \emptyset.$$

Proof. The proof is conducted by contradiction. So suppose that

$$\exists w \in K_{\hat{u}} \text{ such that } \|G_j w\|_2 = 0, \forall j \in \hat{J}_0^c. \quad (2.15)$$

By H3, we have $G_j \neq 0, \forall j \in \hat{J}_0^c$ so that (2.15) makes sense. Combining (2.15) and the definition of $K_{\hat{u}}$ in (2.13) shows that $G_j w = 0, \forall j \in \hat{J}_0^c \cup \hat{J}_0$, i.e.

$$w \in \ker(G).$$

Using H2, we know that for any $w \in \ker(G)$,

$$\exists i \in \hat{I}_0^c \text{ such that } \langle a_i, w \rangle \neq 0.$$

Using the definition of $K_{\hat{u}}$ yet again entails that $w \notin K_{\hat{u}}$. It follows that (2.15) is false. Hence the statement of the lemma. \square

REMARK 2. Note that whenever $G_j \hat{u} \neq 0$ and $G_j w \neq 0$, for $j \in \hat{J}_0^c$ and $w \in K_{\hat{u}} \setminus \{0\}$,

$$\frac{\|G_j w\|_2^2 \|G_j \hat{u}\|_2^2}{\langle G_j \hat{u}, G_j w \rangle^2} > 1.$$

Indeed, $\hat{u} \in \mathcal{K}_{\hat{u}}$ and $w \in K_{\hat{u}} \setminus \{0\}$, $\mathcal{K}_{\hat{u}} \neq K_{\hat{u}}$ so by Schwarz's inequality we have $|\langle \mathbf{G}_j \hat{u}, \mathbf{G}_j w \rangle| < \|\mathbf{G}_j w\|_2 \|\mathbf{G}_j \hat{u}\|_2$. This remark is behind the condition (b) in the proposition below.

PROPOSITION 2.4. Consider \mathcal{F} of the form (2.1). Let the assumptions H2, H3, H4, H5 and H6 hold. For $v \in \mathbb{R}^q \setminus \{0\}$, let \hat{u} be a (local) minimizer of \mathcal{F} such that $\widehat{\mathcal{J}}_0 \subsetneq J$. Put

$$\tau \stackrel{\text{def}}{=} \min_{j \in \widehat{\mathcal{J}}_0^c} \|\mathbf{G}_j \hat{u}\|_2 > 0.$$

We adopt the notations introduced in (2.12) and (2.13) and suppose that $\dim(K_{\hat{u}}) \geq 1$. Assume the following:

(a) there is a constant $C > 1$ such that

$$w \in K_{\hat{u}} \setminus \{0\} \Rightarrow \frac{\|\mathbf{G}_j w\|_2^2 \|\mathbf{G}_j \hat{u}\|_2^2}{\langle \mathbf{G}_j \hat{u}, \mathbf{G}_j w \rangle^2} \leq C, \quad \forall j \in \widehat{\mathcal{J}}_0^c(w),$$

where $\widehat{\mathcal{J}}_0^c(w)$ is as defined in Lemma 2.3 ;

(b) $\varphi''(t) + (C - 1) \frac{\varphi'(t)}{t} < 0$ for all $t > \tau$.

Then the function F given in (2.14) satisfies

$$\langle D^2 F(\hat{u})w, w \rangle < 0, \quad \forall w \in K_{\hat{u}} \setminus \{0\}.$$

Proof. Using Lemma 2.1 and H4, for any $i \in \widehat{\mathcal{I}}_0^c$ and $j \in \widehat{\mathcal{J}}_0^c$, the first and second order differentials $D\psi_i$, $D^2\psi_i$, $D\phi_j$ and $D^2\phi_j$ are well defined on $B(\hat{u}, \rho)$. Then for any $w \in \mathbb{R}^p$ we have¹

$$i \in \widehat{\mathcal{I}}_0^c \Rightarrow \begin{cases} D\psi_i(\hat{u})w & = \text{sign}(\langle a_i, \hat{u} \rangle - v[i]) \langle a_i, w \rangle ; \\ \langle D^2\psi_i(\hat{u})w, w \rangle & = 0 ; \end{cases} \quad (2.16)$$

$$j \in \widehat{\mathcal{J}}_0^c \Rightarrow \begin{cases} D\phi_j(\hat{u})w & = \varphi'(\|\mathbf{G}_j \hat{u}\|_2) \frac{\langle \mathbf{G}_j \hat{u}, \mathbf{G}_j w \rangle}{\|\mathbf{G}_j \hat{u}\|_2} ; \\ \langle D^2\phi_j(\hat{u})w, w \rangle & = \varphi''(\|\mathbf{G}_j \hat{u}\|_2) \left(\frac{\langle \mathbf{G}_j \hat{u}, \mathbf{G}_j w \rangle}{\|\mathbf{G}_j \hat{u}\|_2} \right)^2 \\ & + \varphi'(\|\mathbf{G}_j \hat{u}\|_2) \frac{\|\mathbf{G}_j w\|_2^2 \|\mathbf{G}_j \hat{u}\|_2^2 - \langle \mathbf{G}_j \hat{u}, \mathbf{G}_j w \rangle^2}{\|\mathbf{G}_j \hat{u}\|_2^3} . \end{cases} \quad (2.17)$$

Combining H6 with the assumptions of the proposition, we derive the following chain

¹Note that if $i \in \widehat{\mathcal{I}}_0^c$ then

$$\langle D^2\psi_i(\hat{u})w, w \rangle = \lim_{t \rightarrow 0} \frac{\text{sign}(\langle a_i, \hat{u} + tw \rangle - v[i]) \langle a_i, w \rangle - \text{sign}(\langle a_i, \hat{u} \rangle - v[i]) \langle a_i, w \rangle}{t} = 0.$$

of inequalities:

$$\begin{aligned}
& \langle D^2F(\hat{u})w, w \rangle \\
&= \beta \sum_{i \in \hat{J}_0^c} \varphi''(\|G_j \hat{u}\|_2) \left(\frac{\langle G_j \hat{u}, G_j w \rangle}{\|G_j \hat{u}\|_2} \right)^2 \\
&+ \beta \sum_{i \in \hat{J}_0^c} \varphi'(\|G_j \hat{u}\|_2) \frac{\|G_j w\|_2^2 \|G_j \hat{u}\|_2^2 - \langle G_j \hat{u}, G_j w \rangle^2}{\|G_j \hat{u}\|_2^3} \\
(\text{Lemma 2.3}) &= \beta \sum_{i \in \hat{J}_0^c(w)} \varphi''(\|G_j \hat{u}\|_2) \left(\frac{\langle G_j \hat{u}, G_j w \rangle}{\|G_j \hat{u}\|_2} \right)^2 \\
&+ \beta \sum_{i \in \hat{J}_0^c(w)} \left(\frac{\varphi'(\|G_j \hat{u}\|_2) \|G_j w\|_2^2 \|G_j \hat{u}\|_2^2}{\|G_j \hat{u}\|_2 \langle G_j \hat{u}, G_j w \rangle^2} - \frac{\varphi'(\|G_j \hat{u}\|_2)}{\|G_j \hat{u}\|_2} \right) \left(\frac{\langle G_j \hat{u}, G_j w \rangle}{\|G_j \hat{u}\|_2} \right)^2 \\
\text{by (a)} &\leq \beta \sum_{i \in \hat{J}_0^c(w)} \left(\varphi''(\|G_j \hat{u}\|_2) + \frac{\varphi'(\|G_j \hat{u}\|_2)}{\|G_j \hat{u}\|_2} (C-1) \right) \left(\frac{\langle G_j \hat{u}, G_j w \rangle}{\|G_j \hat{u}\|_2} \right)^2 \\
\text{by (b)} &< 0, \quad \forall w \in K_{\hat{u}} \setminus \{0\}.
\end{aligned}$$

One can easily check that the same result holds true if $\hat{I}_0^c = \emptyset$. The proof is complete. \square

REMARK 3. If $C = 2$, assumption (a) in Proposition 2.4 is satisfied by the PF (f1) in Table 2.1 for $t > 1/\alpha$ and by the PF (f2) for $t > 1/(-\ln \alpha) > 0$. These PFs are bounded above. This assumption is not satisfied by the PFs (f3) and (f4) in Table 2.1 for any $\tau \geq 0$.

PROPOSITION 2.5. Consider \mathcal{F} of the form (2.1) where $G_j : \mathbb{R}^p \rightarrow \mathbb{R}$ for all $j \in J$ (i.e. $s = 1$). Let the assumptions H2, H3, H4, H5 and H6 hold. For $v \in \mathbb{R}^q$, let \hat{u} be a (local) minimizer of \mathcal{F} such that $\hat{J}_0 \subsetneq J$. We adopt the notations introduced in (2.12) and (2.13) and suppose that $\dim(K_{\hat{u}}) \geq 1$. Then the function F given in (2.14) satisfies

$$\langle D^2F(\hat{u})w, w \rangle < 0, \quad \forall w \in K_{\hat{u}} \setminus \{0\}.$$

Proof. We can denote $\|G_j u\|_2 = |G_j u|$ since $G_j \in \mathbb{R}^{1 \times p}$. In this case (2.17) reads:

$$j \in \hat{J}_0^c \Rightarrow \begin{cases} D\phi_j(\hat{u})w &= \varphi'(|G_j \hat{u}|) \frac{G_j \hat{u} G_j w}{|G_j \hat{u}|} = \varphi'(|G_j \hat{u}|) \text{sign}(G_j \hat{u}) G_j w \\ \langle D^2\phi_j(\hat{u})w, w \rangle &= \varphi''(|G_j \hat{u}|) (G_j w)^2 \end{cases}$$

Using (2.16), Lemma 2.3 and H6, we find

$$\langle D^2F(\hat{u})w, w \rangle = \beta \sum_{i \in \hat{J}_0^c} \varphi''(|G_j \hat{u}|) (G_j w)^2 < 0, \quad \forall w \in K_{\hat{u}} \setminus \{0\}.$$

Hence the conclusion. \square

PROPOSITION 2.6. Consider \mathcal{F} of the form (2.1). Let the assumptions H2, H3, H4, H5 and H6 hold. If $s \geq 2$, we add assumptions (a) and (b) of Proposition 2.4 (see p. 9). For $v \in \mathbb{R}^q \setminus \{0\}$, let \hat{u} be a (local) minimizer of \mathcal{F} . Then

$$\mathcal{K}_{\hat{u}} = \{\hat{u}\} \quad \text{and} \quad K_{\hat{u}} = \{0\}. \quad (2.18)$$

Proof. Suppose that $\dim(K_{\hat{u}}) \geq 1$.

Observe that \mathcal{F} in (2.1) can be rewritten as

$$\mathcal{F}(\hat{u}) = \sum_{i \in \hat{I}_0} |\langle a_i, \hat{u} \rangle - v[i]| + \beta \sum_{i \in \hat{J}_0} \varphi(\|G_i \hat{u}\|_2) + F(\hat{u}), \quad (2.19)$$

where F is given in (2.14). The first two sums of the equation above are null, so

$$\mathcal{F}(\hat{u}) = F(\hat{u}).$$

From the definition of $K_{\hat{u}}$ in (2.13), we have

$$w \in K_{\hat{u}} \Rightarrow \begin{cases} \langle a_i, \hat{u} + w \rangle = \langle a_i, \hat{u} \rangle = v[i] & \forall i \in \hat{I}_0 \\ \|G_j(\hat{u} + w)\|_2 = \|G_j \hat{u}\|_2 = 0 & \forall j \in \hat{J}_0 \end{cases}. \quad (2.20)$$

In particular,

$$\hat{u} + w \in K_{\hat{u}}, \quad \forall w \in K_{\hat{u}}.$$

Hence,

$$\begin{aligned} w \in K_{\hat{u}} \Rightarrow \mathcal{F}(\hat{u} + w) &= \sum_{i \in \hat{I}_0^c} |\langle a_i, \hat{u} + w \rangle - v[i]| + \beta \sum_{i \in \hat{J}_0^c} \varphi(\|G_i(\hat{u} + w)\|_2) \\ &= F(\hat{u} + w). \end{aligned} \quad (2.21)$$

Since \mathcal{F} has a (local) minimum at \hat{u} , there is $0 < \varrho \leq \rho$, for $\rho > 0$ as given in Lemma 2.1, such that

$$w \in K_{\hat{u}} \cap B(0, \varrho) \Rightarrow \mathcal{F}(\hat{u}) \leq \mathcal{F}(\hat{u} + w).$$

Combining this with (2.21) yields

$$w \in K_{\hat{u}} \cap B(0, \varrho) \Rightarrow F(\hat{u}) = \mathcal{F}(\hat{u}) \leq \mathcal{F}(\hat{u} + w) = F(\hat{u} + w). \quad (2.22)$$

This shows that F has a (local) minimum at \hat{u} since F is the restriction of \mathcal{F} on $K_{\hat{u}} \cap B(\hat{u}, \varrho)$. Then F must satisfy the second-order necessary condition for a (local) minimum, namely $\langle D^2 F(\hat{u})w, w \rangle \geq 0, \forall w \in K_{\hat{u}}$. However, by Propositions 2.4 and 2.5, we know that

$$\langle D^2 F(\hat{u})w, w \rangle < 0, \quad \forall w \in K_{\hat{u}} \setminus \{0\},$$

which contradicts the fact that \hat{u} is a (local) minimizer of \mathcal{F} and F .

Since $F(\hat{u})$ is well defined, the only possibility for \hat{u} to be a (local) minimizer of \mathcal{F} is that $w = 0, \forall w \in K_{\hat{u}}$. Using the definition of $K_{\hat{u}}$ in (2.13) yet again, the latter means that we must have the implication given below:

$$\begin{cases} \langle a_i, w \rangle = 0 & \forall i \in \hat{I}_0, \\ G_j w = 0 & \forall j \in \hat{J}_0, \end{cases} \Rightarrow w = 0. \quad (2.23)$$

Let us denote

$$\hat{I}_0 = \{i_1, \dots, i_{\#\hat{I}_0}\} \quad \text{and} \quad \hat{J}_0 = \{j_1, \dots, j_{\#\hat{J}_0}\}.$$

Then define the following matrices:

$$A_0 = \begin{bmatrix} a_{i_1}^T \\ \vdots \\ a_{\#\hat{I}_0}^T \end{bmatrix} \in \mathbb{R}^{\#\hat{I}_0 \times p} \quad \text{and} \quad G_0 = \begin{bmatrix} G_{j_1} \\ \vdots \\ G_{\#\hat{J}_0} \end{bmatrix} \in \mathbb{R}^{\#\hat{J}_0 s \times p}, \quad (2.24)$$

as well as

$$H_0 = \begin{bmatrix} A_0 \\ G_0 \end{bmatrix} \in \mathbb{R}^{(\#\hat{I}_0 + \#\hat{J}_0 s) \times p}. \quad (2.25)$$

For any integer $m \geq 0$ let \mathbb{O}_m be the m -length column vector composed of zeros:

$$\mathbb{O}_m = [0, \dots, 0]^T \in \mathbb{R}^m.$$

Define also the $(\#\hat{I}_0 + \#\hat{J}_0 s)$ -length column vector v_0 by

$$v_0 = [v[i_1], \dots, v[\#\hat{I}_0], \mathbb{O}_{\#\hat{J}_0 s}^T]^T.$$

Using these notations, $\mathcal{K}_{\hat{u}}$ in (2.12) and $K_{\hat{u}}$ in (2.13) equivalently read

$$\begin{aligned} \mathcal{K}_{\hat{u}} &= \{w \in \mathbb{R}^p : H_0 w = v_0\}; \\ K_{\hat{u}} &= \{w \in \mathbb{R}^p : H_0 w = \mathbb{O}_{(\#\hat{I}_0 + \#\hat{J}_0 s)}\}. \end{aligned}$$

Then the implication stated in (2.23) equivalently reads

$$H_0 w = 0 \quad \Rightarrow \quad w = 0 \in \mathbb{R}^p. \quad (2.26)$$

It is well known that (2.26) cannot hold unless

$$\text{rank}(H_0) = p.$$

Consequently, $K_{\hat{u}} = \{0\}$ and $\dim(K_{\hat{u}}) = 0$. Moreover, \hat{u} is the unique solution of the matrix equation given below

$$H_0 \hat{u} = v_0. \quad (2.27)$$

Then $\mathcal{K}_{\hat{u}}$ in (2.12) reads

$$\mathcal{K}_{\hat{u}} = \{\hat{u}\}.$$

The proof is complete. \square

Proof of Theorem 2.2. When $s \geq 2$, we have to notice that each G_{j_k} composing G_0 as given in (2.24) is of the form

$$G_{j_k} = \begin{bmatrix} G_{j_k}^1 \\ \vdots \\ G_{j_k}^s \end{bmatrix} \in \mathbb{R}^{s \times p}.$$

Since \hat{u} is well defined as the unique solution of (2.27), all its entries $\hat{u}[k]$, $1 \leq k \leq p$ are well defined. This cannot hold true unless for every $k \in \{1, \dots, p\}$ we have at least an $i \in \hat{I}_0$ such that $a_i[k] \neq 0$ or a $j \in \hat{J}_0$ and $1 \leq \ell \leq s$ such that $G_{j_k}^\ell[k] \neq 0$. Hence the result stated in (2.11).

The fact that \mathcal{F} has a strict minimum at \hat{u} comes from the fact that the equations in (2.27) admits a unique solution which is exactly \hat{u} . \square

3. Minimization Methods. The minimization of nonconvex nonsmooth energy \mathcal{F} given by (2.1) involves three major difficulties that drastically restrict the methods that can be envisaged. Because of the nonconvexity of φ , \mathcal{F} may exhibit a large number of local minima which are not global. In addition, \mathcal{F} is nonsmooth at the minimizers (see section 2), and thus usual gradient-based methods are inappropriate even for local minimization. Finally, the matrix A can have numerous nonzero elements beyond the diagonal and is often ill-conditioned. In [25], a nonsmooth GNC continuation method is inaugurated to solve a nonconvex nonsmooth minimization problem where \mathcal{F} is similar of the form (2.1) except the data fitting term is ℓ_2 -norm. Here our goal is to conceive nonsmooth GNC schemes for \mathcal{F} of the form given by (2.1). The experimental results in [25] showed that the resultant method provides better performance with significantly smaller computational cost, compared to a simulated annealing method.

Consider a sequence

$$\varepsilon_0 = 0 < \varepsilon_1 < \dots < \varepsilon_k < \dots < \varepsilon_n = 1. \quad (3.1)$$

We approach φ by a sequence of $\varphi_\varepsilon : \mathbb{R} \rightarrow \mathbb{R}_+$ such that φ_0 is convex and φ_ε monotonously reaches φ when ε goes from 0 to 1 in (3.1), with $\varphi_1 = \varphi$ and φ_ε is nonsmooth at 0 for any $\varepsilon \in [0, 1]$. (To simplify the notations, we write ε for ε_k whenever this is clear from the context.) Correspondingly, our energy \mathcal{F} is approximated by a sequence \mathcal{F}_ε as given below:

$$\mathcal{F}_\varepsilon(u) = \|Au - v\|_1 + \beta \sum_{j \in J} \varphi_\varepsilon(\|G_j u\|_2), \quad 0 \leq \varepsilon \leq 1. \quad (3.2)$$

Thus \mathcal{F}_0 is convex (and nonsmooth), \mathcal{F}_ε monotonously goes to \mathcal{F} when ε increases and we have $\mathcal{F}_1 = \mathcal{F}$.

Based on the assumptions H4-H6, we can rewrite φ_ε as follows

$$\varphi_\varepsilon(t) = \psi_\varepsilon(t) + \alpha_\varepsilon |t| \quad \text{where} \quad \alpha_\varepsilon = \varphi'_\varepsilon(0^+). \quad (3.3)$$

We see that φ_ε in (3.3) is composed of two terms: the first one ψ_ε is \mathcal{C}^2 -smooth and concave whereas the second one $\alpha_\varepsilon |t|$ is convex and nonsmooth at zero. Decomposing \mathcal{F}_ε in (3.2) according to (3.3) yields:

$$\mathcal{F}_\varepsilon(u) = \|Au - v\|_1 + \beta \Psi_\varepsilon(u) + \beta \alpha_\varepsilon \sum_{j \in J} \|G_j u\|_2 \quad (3.4)$$

$$\text{where} \quad \Psi_\varepsilon(u) = \sum_{j \in J} \psi_\varepsilon(\|G_j u\|_2).$$

Our approach to tackle the difficulties for minimizing the function \mathcal{F}_ε in (3.4) is to apply variable-splitting and penalty techniques to separate the nonconvex term and the nonsmooth term using additional variables. In the following, we propose a numerical scheme to minimize \mathcal{F}_ε in (3.4) for every $\varepsilon \in [0, 1]$. The minimizer u of \mathcal{F}_1 provides the sought-after approximation of the global minimizer of \mathcal{F} .

3.1. Numerical scheme based on fitting to Gu . Here we derive a numerical method to minimize (3.4). It is based on variable-splitting and penalty technique to transfer the nonsmooth term out of $\mathcal{F}_{\varepsilon_k}$ in such a way that the TV denoising step can be done by a shrinkage operation, as proposed in [30]. To this end, we consider an

augmented energy $\mathcal{J}_{\varepsilon_k} : \mathbb{R}^p \times \mathbb{R}^q \times \mathbb{R}^{sp} \rightarrow \mathbb{R}$ which involves a fitting of the auxiliary variables $z \in \mathbb{R}^{sp}$ to Gu and $w \in \mathbb{R}^q$ to Au :

$$\mathcal{J}_{\varepsilon_k}(u, w, z) = \gamma \|Au - w\|_2^2 + \|w - v\|_1 + \beta \Psi_{\varepsilon_k}(u) + \gamma \|Gu - z\|_2^2 + \beta \alpha_{\varepsilon_k} \sum_{j \in J} \|z_j\|_2, \quad (3.5)$$

where $\gamma > 0$ and $z_j \in \mathbb{R}^s$ for all $j \in J$. For u and w fixed, $\mathcal{J}_{\varepsilon_k}(u, w, \cdot)$ is convex and non-differentiable because of the term $\sum_j \|z_j\|_2$. For u and z fixed, $\mathcal{J}_{\varepsilon_k}(u, \cdot, z)$ is convex and non-differentiable because of the term $\|w - v\|_1$. Here both terms $\|Au - w\|_2^2$ and $\|Gu - z\|_2^2$ are weighted by γ . In the proposed iterative algorithm, we will make γ larger and larger so that w comes close enough to Au and z close enough to Gu .

Given w and z , the function $u \mapsto \mathcal{J}_{\varepsilon_k}(u, w, z)$ is twice differentiable and nonconvex so that it can be minimized by gradient-based methods. The computational steps are given as follows:

$$\begin{aligned} z^{(l,k)} &= \arg \min_{z \in \mathbb{R}^{sp}} \mathcal{J}_{\varepsilon_k}(u^{(l-1,k)}, w^{(l-1,k)}, z) \\ &= \arg \min_{z \in \mathbb{R}^{sp}} \left\{ \sum_{j \in J} \left(\gamma \|G_j u^{(l-1,k)} - z_j\|_2^2 + \beta \alpha_{\varepsilon} \|z_j\|_2 \right) \right\} \end{aligned} \quad (3.6)$$

$$\begin{aligned} w^{(l,k)} &= \arg \min_{w \in \mathbb{R}^q} \mathcal{J}_{\varepsilon_k}(u^{(l-1,k)}, w, z^{(l,k)}) \\ &= \arg \min_{w \in \mathbb{R}^q} \left\{ \gamma \|Au^{(l-1,k)} - w\|_2^2 + \|w - v\|_1 \right\} \end{aligned} \quad (3.7)$$

$$\begin{aligned} u^{(l,k)} &= \arg \min_{u \in \mathbb{R}^p} \mathcal{J}_{\varepsilon_k}(u, w^{(l,k)}, z^{(l,k)}) \\ &= \arg \min_{u \in \mathbb{R}^p} \left\{ \gamma \|Au - w^{(l,k)}\|_2^2 + \beta \Psi_{\varepsilon}(u) + \gamma \|Gu - z^{(l,k)}\|_2^2 \right\} \end{aligned} \quad (3.8)$$

In this case, we initialize with $u^{(0,k)} \stackrel{\text{def}}{=} u_{\varepsilon_{k-1}}$ where $u_{\varepsilon_{k-1}}$ results from the minimization of $\mathcal{J}_{\varepsilon_{k-1}}$ with respect to u . We remark that $w^{(l-1,k)}$ is not required in the computation in (3.6).

3.1.1. Computation of $z^{(l,k)}$ according to (3.6). Solving (3.6) amounts to solve p independent problems:

$$z_i^{(l,k)} = \arg \min_{z_j \in \mathbb{R}^s} \left\{ \gamma \|G_j u^{(l-1,k)} - z_j\|_2^2 + \beta \alpha_{\varepsilon} \|z_j\|_2 \right\}, \quad \forall j \in J. \quad (3.9)$$

As shown in [30, pp.251-252], each one of the problems in (3.9) can be solved efficiently using s -dimensional shrinkage:

$$z_j^{(l,k)} = \frac{G_j u^{(l-1,k)}}{\|G_j u^{(l-1,k)}\|} \max \left\{ \|G_j u^{(l-1,k)}\|_2 - \frac{\beta \alpha_{\varepsilon_k}}{2\gamma}, 0 \right\}, \quad \forall j \in J. \quad (3.10)$$

3.1.2. Computation of $w^{(l,k)}$ according to (3.7). The task is similar to the computation of $z^{(l,k)}$. The solution in (3.7) can be found as follows:

$$w_i^{(l,k)} = \frac{Au^{(l-1,k)} - v}{\|Au^{(l-1,k)} - v\|} \max \left\{ \|Au^{(l-1,k)} - v\|_2 - \frac{1}{2\omega}, 0 \right\}, \quad \forall i \in I. \quad (3.11)$$

3.1.3. Computation of $u^{(l,k)}$ according to (3.8). For $\varepsilon_0 = 0$ ($k = 0$), the finding of $u^{(l,0)}$ amounts to minimize the convex quadratic function:

$$\min_{u \in \mathbb{R}^p} \left\{ \gamma \|Au - w^{(l,0)}\|_2^2 + \gamma \|Gu - z^{(l,0)}\|_2^2 \right\}.$$

For $\varepsilon_k > 0$, the Quasi-Newton method can be used to solve (3.8). Since all the terms in $\mathcal{J}_{\varepsilon_k}(\cdot, w^{(l,k)}, z^{(l,k)})$ are twice differentiable, we can find out the corresponding gradient vector $\nabla_u \mathcal{J}_{\varepsilon_k} \stackrel{\text{def}}{=} \nabla_u \mathcal{J}_{\varepsilon_k}(u, w^{(l,k)}, z^{(l,k)})$ and the Hessian $\nabla_u^2 \mathcal{J}_{\varepsilon_k} \stackrel{\text{def}}{=} \nabla_u^2 \mathcal{J}_{\varepsilon_k}(u, w^{(l,k)}, z^{(l,k)})$ of $\mathcal{J}_{\varepsilon_k}(\cdot, w^{(l,k)}, z^{(l,k)})$ to tackle the minimization problem:

$$\nabla_u \mathcal{J}_{\varepsilon_k} = 2\gamma A^T (Au - w^{(l,k)}) + \beta \nabla \nabla_u \Psi_{\varepsilon_k}(u) + 2\gamma (G^T G u - z^{(l,k)}) \quad (3.12)$$

and

$$\nabla_u^2 \mathcal{J}_{\varepsilon_k} = 2\gamma A^T A + 2\gamma G^T G + \beta \nabla_u^2 \Psi_{\varepsilon_k}(u). \quad (3.13)$$

where $\nabla_u^2 \Psi_{\varepsilon_k}(u) \stackrel{\text{def}}{=} \nabla_u^2 \Psi_{\varepsilon_k}(u, w^{(l,k)}, z^{(l,k)})$ of $\Psi_{\varepsilon_k}(\cdot, w^{(l,k)}, z^{(l,k)})$. Since $\nabla_u^2 \Psi_{\varepsilon_k}(u)$ is negative definite, the Hessian $\nabla_u^2 \mathcal{J}_{\varepsilon_k}$ may be not positive definite. This may prevent the Quasi-Newton method from convergence as the resultant search direction may not be a descent direction. In order to ensure the descent direction, we simply use the positive definite part of the Hessian matrix in the optimization procedure. Such procedure can guarantee that the proposed algorithm is a descent method for the minimization problem. Thanks to the term $2\gamma G^T G$, the coefficient matrix $2\gamma A^T A + 2\gamma G^T G$ is always positive definite because of $\ker A \cap \ker G = \{0\}$ stated in (1). The solution can be updated by

$$u^{(l,k)} = u^{(l-1,k)} + \tau \Delta u^{(l,k)}$$

where $\tau > 0$ is the step-size and $\Delta u^{(l,k)}$ is found by solving

$$(2\gamma A^T A + 2\gamma G^T G) \Delta u^{(l,k)} = -\nabla_u \mathcal{J}_{\varepsilon_k}. \quad (3.14)$$

We remark in image restoration that A is usually a blurring matrix generated by a symmetric point spread function. The computational cost of the method is dominated by three fast discrete transforms in solving the linear system in (3.14), see [20]. The computational cost for each fast transform is only $O(p \log p)$ for a $p \times p$ blurring matrix A [20].

Three different strategies to determine the step-size τ were tested: Armijo rule, Goldstein rule and a fixed τ [26, Chapter 3]. By observing experimental results, we found out that the numerical schemes based on these three rules converged to the same solutions, while using the first two rules required heavy additional computation cost. Therefore, we fixed $\tau = 1$ for all of our experiments.

3.2. Algorithm.

Set $\varepsilon_0 = 0$ and $\Delta\varepsilon = 1/n$, and initialize $u^{(0,0)}$.

For $k = 0 \rightarrow n$

 Set $l = 1$, initial value of ω , and $\text{relerr} = \text{tol} + 1$

 While $\text{relerr} > \text{tol}$ do

 Obtain $z^{(l,k)}$ by computing (3.10) and $w^{(l,k)}$ by computing (3.11);

 If $k = 0$

 Solve $(2\gamma A^T A + 2\gamma \sum_{j \in J} G_j^T G_j) u^{(l,k)} = A^T w^{(l,k)} + \gamma \sum_{j \in J} G_j^T z^{(l,k)}$;

Otherwise
 Solve $(2\gamma A^T A + 2\gamma \sum_{j \in J} G_j^T G_j) \Delta u^{(l,k)} = -\nabla_u \mathcal{J}_{\varepsilon_k}$;
 Update $u^{(l,k)} = u^{(l-1,k)} + \tau \Delta u^{(l,k)}$;
 End If;
 Compute $\text{reterr} = \|u^{(l,k)} - u^{(l-1,k)}\|_2 / \|u^{(l,k)}\|_2$;
 End While
 Increase γ and set $l = l + 1$;
 Set $u^{(0,k+1)} = u^{(l,k)}$ (for the initial guess of the next outer loop);
 Update $\varepsilon_{k+1} = \varepsilon_k + \Delta\varepsilon$;
 End For

4. Numerical Examples. In this section, we present the experimental results to demonstrate the efficiency of the algorithm proposed in the last section. Signal to noise ratio (SNR) is used to measure the quality of the restored images. The parameter tol is set to be 10^{-4} in the proposed method. The initial value of γ is set to be 0.1, and its value is updated by 1.3γ at each iteration. The PF used in all the illustrations was also tested in [25]:

$$\varphi(t) = \frac{\alpha|t|}{1 + \alpha|t|}, \quad \varphi_\varepsilon(t) = \frac{\alpha|t|}{1 + \varepsilon\alpha|t|}, \quad 0 \leq \varepsilon \leq 1. \quad (4.1)$$

Note that both φ and φ_ε satisfy all assumptions H4, H5 and H6, see p. 3. In the tests, we use $\alpha = \alpha_\varepsilon = 0.5$. All the computational tasks are performed using MATLAB on a computer with Corel(TM)2 CPU with 2.66 GHz and 1.98GB of RAM.

In the first experiment, we consider to use the proposed algorithm to generate a high-resolution image from a low-resolution image. The aim is to demonstrate that the generated high-resolution image pixels can fit low-resolution image pixels exactly. The original testing image is the picture of Lena of size 256×256 as shown in Figure 4.1(a). To generate a low-resolution image, we take the pixels from the original image by downsampling of factor 2. The observed image of size 128×128 is shown in Figure 4.1(b) and its gray values are in $[0, 1]$. Here we employ the discrete form of the Laplacian operator given by

$$\begin{bmatrix} 0 & -1 & 0 \\ -1 & 4 & -1 \\ 0 & -1 & 0 \end{bmatrix}.$$

The resulting high-resolution image of size 256×256 generated by the proposed algorithm is shown in Figure 4.2. All observed pixels are faithfully fitted by the relevant pixels of the restored image since their average difference is 1.28×10^{-6} , with a maximum difference 1×10^{-4} (i.e. the precision given by the parameter tol). This result corroborates the theory in Section 2 and shows that the proposed algorithm can match the observed samples quite exactly.

In the second experiment, we compare the proposed method with the TVL1 method [30]. The linear systems in (3.14) can be solved by fast discrete transforms in the proposed method. The testing image is the modified Shepp-Logan image of size 128×128 . To generate the observed images, we added impulsive noise with 10%, 20% and 30% with blurring. The blurring function is chosen to be a two dimensional truncated gaussian function

$$h(s, t) = \exp\left(\frac{-s^2 - t^2}{2\sigma^2}\right), \quad \text{for } -3 \leq s, t \leq 3,$$



FIG. 4.1. (a) The original high-resolution image and (b) the low-resolution image.



FIG. 4.2. The resulting high-resolution image by the proposed method.

with $\sigma = 1.5$. Different initial guesses have been considered, including the observed image, the least squares solution and a flat image (all the pixel values are 0.5). From our experimental results, the proposed method is not insensitive to all of the initial guesses. Therefore, we only demonstrate the results which the initial guesses are the observed images. In the experiments we test different values of β in order to find out the restored image with the highest SNR among the tested values. Similarly, we also test different values of the regularization parameter in the TVL1 [30] to find out the restored image with the highest SNR.

Figure 4.3(a) shows the original images. Figures 4.3(b)-(d) show their corresponding images with blur and noise as described in the above settings respectively. Figures 4.4(a)-(c) show the images restored by the proposed method, and Figures 4.4(d)-(f) show the images restored by the TVL1 method. We see from the figures that the images restored by the proposed method are visually better than those by the TVL1 method. In Figures 4.5 (the 40th row of the image) and 4.6 (the 40th column of the image), we display two 1-dimensional sections of the restored images by the proposed method and the TVL1 method. We see that the proposed method is more effective for restoring images with constant regions surrounded by closed contours. The SNRs of the restored images by the proposed method are 45.01dB, 40.73dB and 35.40dB for 10%, 20% and 30% impulsive noises respectively. However, the TVL1 method restores images with SNRs 31.80dB, 30.71dB and 27.96dB for 10%, 20% and 30% impulsive

noises respectively.

5. Concluding Remarks. In this paper, we considered image reconstruction and image restoration using ℓ_1 data fitting and nonconvex and nonsmooth regularization on the image. Our theoretical results show that the solutions of the corresponding minimization problem are such that any pixel is involved in a data equation that is fitted exactly or in a null component of the regularization term. This remarkable property can be used in different ways in various imaging problems. From a practical side, we conceived a fast numerical scheme to solve this difficult minimization problem. Experimental results have shown the effectiveness of the proposed numerical scheme.

REFERENCES

- [1] G. Aubert and P. Kornprobst, *Mathematical Problems in Image Processing*, Springer-Verlag, Berlin, 2nd ed., 2006.
- [2] J.-F. Aujol, G. Gilboa, T. Chan and S. Osher, "Structure-Texture Image Decomposition - Modeling, Algorithms, and Parameter Selection", *International Journal of Computer Vision*, 67(1), pp. 111-136, 2006.
- [3] L. Bar, A. Brook, N. Sochen and N. Kiryati, "Deblurring of color images corrupted by salt-and-pepper noise", *IEEE Trans. on Image Processing*, 16(4), 2007, pp. 1101-1111.
- [4] J. E. Besag, "Digital image processing: towards Bayesian image analysis," *J. Appl. Stat.*, 16(3), 1989, pp. 395-407.
- [5] M. Black and A. Rangarajan, "On the unification of line processes, outlier rejection, and robust statistics with applications to early vision," *International J. of Computer Vision*, vol. 19(1), 1996, pp. 57-91.
- [6] P. G. Ciarlet, *Introduction to Numerical Linear Algebra and Optimization*, Cambridge University Press, 1989.
- [7] G. Demoment, "Image reconstruction and restoration: Overview of common estimation structure and problems," *IEEE Trans. Acoustics Speech and Signal Processing*, vol. ASSP-37(12), 1989, pp. 2024-2036.
- [8] S. Durand and M. Nikolova, "Denoising of frame coefficients using ℓ_1 data-fidelity term and edge-preserving regularization," *SIAM J. on Multiscale Modeling and Simulation*, 6(2), 2007, pp. 547-576.
- [9] H. Fu, M. Ng, M. Nikolova, and J. Barlow, "Efficient minimization methods of mixed ℓ_2 - ℓ_1 and ℓ_1 - ℓ_1 norms for image restoration," *SIAM J. Sci. Comput.*, 27(6), 2006, pp. 1881-1902.
- [10] D. Geman and G. Reynolds, "Constrained restoration and recovery of discontinuities," *IEEE Trans. Pattern Anal. Machine Intell.*, PAMI-14(3), 1992, pp. 367-383.
- [11] D. Geman and C. Yang, "Nonlinear image recovery with half-quadratic regularization," *IEEE Trans. on Image Processing*, 4(7), 1995, pp. 932-946.
- [12] S. Geman and D. Geman, "Stochastic relaxation, Gibbs distributions, and the Bayesian restoration of images," *IEEE Trans. Pattern Anal. Machine Intell.*, PAMI-6(6), 1984, pp. 721-741.
- [13] R. Gonzalez and R. Woods, "Digital Image Processing," Pearson Int. Edition, 3rd ed., 2008.
- [14] P. J. Green, "Bayesian reconstructions from emission tomography data using a modified EM algorithm," *IEEE Trans. Med. Imag.*, vol. 9(1), 1990, pp. 84-93.
- [15] X. Guo, F. Li and M. Ng, "A fast ℓ_1 -TV algorithm for image restoration", *SIAM Journal on Scientific Computing*, 31(3), 2009, pp. 2322-2341.
- [16] A. Jain, *Fundamentals of Digital Image Processing*, Prentice-Hall, Englewood Cliffs, NJ, 1989.
- [17] K. Lange, "Convergence of EM image reconstruction algorithms with Gibbs priors," *IEEE Trans. Med. Imag.*, 9(4), 1990, pp. 439-446.
- [18] S. Li, *Markov Random Field Modeling in Computer Vision*, Springer-Verlag, New York, 1st ed., 1995.
- [19] D. Mumford and J. Shah, "Boundary detection by minimizing functionals," *Proceedings of the IEEE Int. Conf. on Acoustics, Speech and Signal Processing*, pp. 22-26, 1985.
- [20] M. K. Ng, R. H. Chan, and W. Tang, "A fast algorithm for deblurring models with Neumann boundary conditions," *SIAM J. Sci. Comput.*, 21(3), 1999, pp. 851-866.
- [21] M. Nikolova, "Markovian reconstruction using a GNC approach," *IEEE Trans. on Image Processing*, 8(9), 1999, pp. 1204-1220.

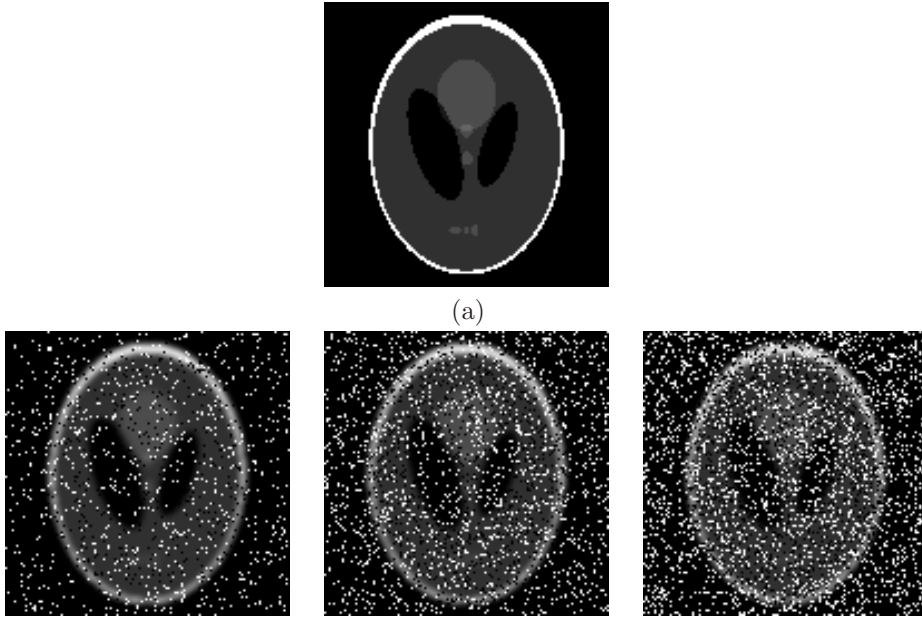


FIG. 4.3. (a) The original image; (b) the observed image of 10% impulsive noise; (c) the observed image of 20% impulsive noise; (d) the observed image of 30% impulsive noise.

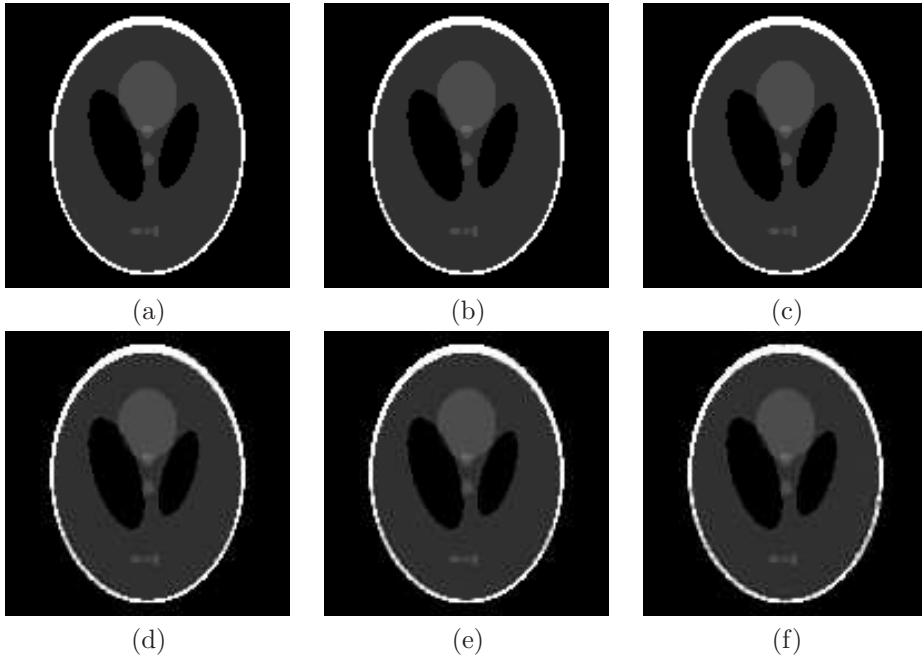


FIG. 4.4. The restored images of (a) 10% impulsive noise ($\beta = 0.04$); (b) 20% impulsive noise ($\beta = 0.03$); (c) 30% impulsive noise ($\beta = 0.06$) by the proposed method. The restored images of (d) 10% impulsive noise ($\beta = 0.02$); (e) 20% impulsive noise ($\beta = 0.02$); (f) 30% impulsive noise ($\beta = 0.03$) by the TVL1 method.

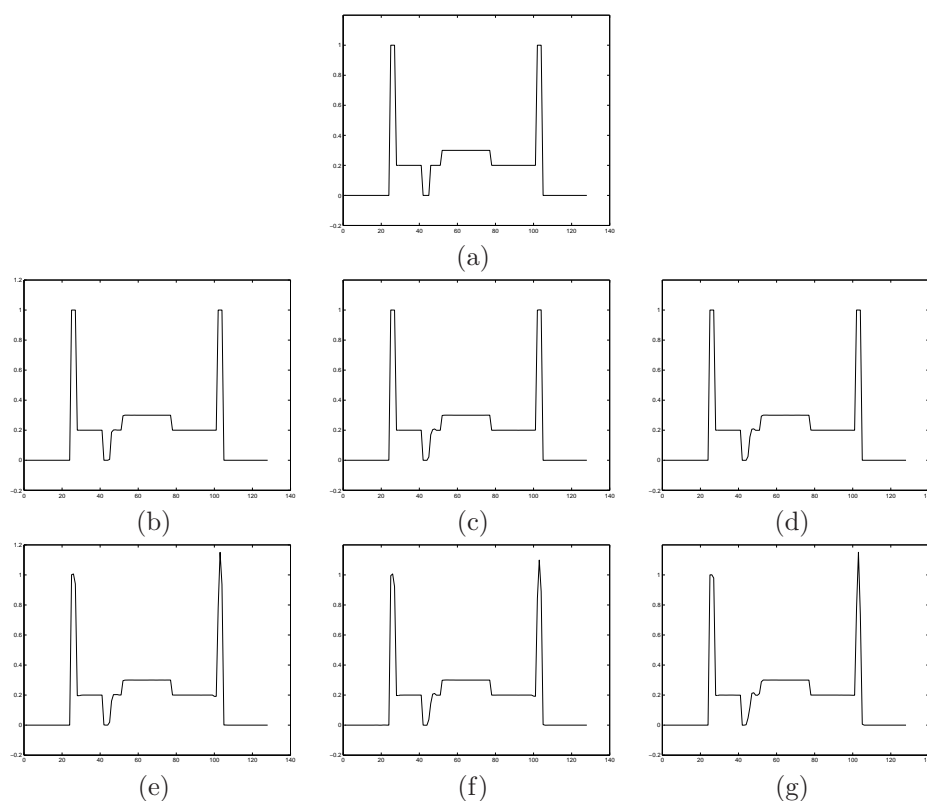


FIG. 4.5. (a) The 1D section (the 40th row) of the original image. the restored 1D section of (b) 10% impulsive noise; (c) 20% impulsive noise; (d) 30% impulsive noise by the proposed method in Figure 4.2; the restored 1D section of (e) 10% impulsive noise; (f) 20% impulsive noise; (g) 30% impulsive noise by the TVL1 method in Figure 4.2.

- [22] M. Nikolova, "Minimizers of cost-functions involving non-smooth data-fidelity terms. Application to the processing of outliers," *SIAM J. on Numerical Analysis*, 40(3), 2002, pp. 965-994.
- [23] M. Nikolova, "A variational approach to remove outliers and impulse noise," *J. of Mathematical Imaging and Vision*, 20(1-2), 2004, pp. 99-120.
- [24] M. Nikolova, "Analysis of the recovery of edges in images and signals by minimizing nonconvex regularized least-squares," *SIAM J. on Multiscale Modeling and Simulation*, 4(3), 2005, pp. 960-991.
- [25] M. Nikolova, M. K. Ng, S. Zhang, and W. Ching, "Efficient reconstruction of piecewise constant images using nonsmooth nonconvex minimization," *SIAM J. Imaging Sciences*, 1(1), 2008, pp. 2-25.
- [26] J. Nocedal and S. Wright, *Numerical Optimization*, Springer, 1999.
- [27] M. Robini, A. Lachal, and I. Magnin, "A stochastic continuation approach to piecewise constant reconstruction", *IEEE Trans. on Image Processing*, 16(10), 2007, pp. 2576-2589.
- [28] R. Stevenson and E. Delp, "Fitting curves with discontinuities," *Proc. of the 1st Int. Workshop on Robust Comput. Vision*, Seattle, WA, 1990, pp. 127-136.
- [29] A. Tikhonov and V. Arsenin, *Solutions of Ill-Posed Problems*, Winston, Washington DC, 1977.
- [30] Y. Wang, J. Yang, W. Yin, and Y. Zhang, "A new alternating minimization algorithm for total variation image reconstruction," *SIAM Journal on Imaging Sciences*, 1(3), 2008, pp. 248-272.

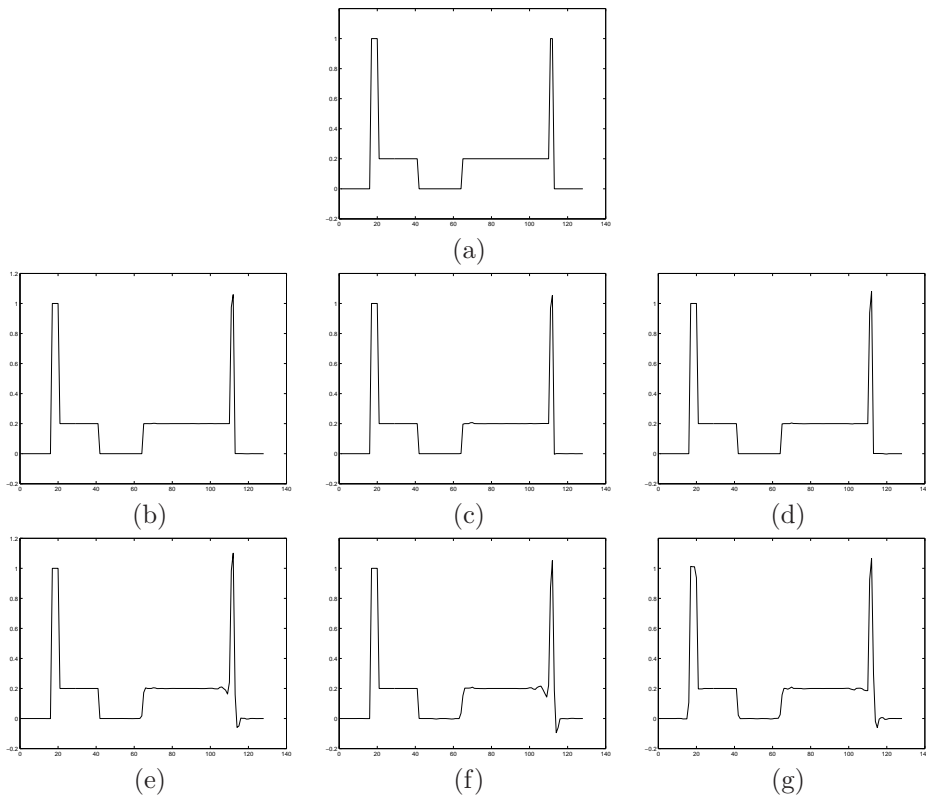


FIG. 4.6. (a) The 1D section (the 40th column) of the original image. the restored 1D section of (b) 10% impulsive noise; (c) 20% impulsive noise; (d) 30% impulsive noise by the proposed method in Figure 4.2; the restored 1D section of (e) 10% impulsive noise; (f) 20% impulsive noise; (g) 30% impulsive noise by the TVL1 method in Figure 4.2.